LETTERS
PUBLISHED ONLINE: 4 JULY 2010 | DOI: 10.1038/NNANO.2010.128
nature nanotechnology

Light-driven nanoscale plasmonic motors

Ming Liu[1], Thomas Zentgraf[1], Yongmin Liu[1], Guy Bartal[1] and Xiang Zhang[1,2]*

When Sir William Crookes developed a four-vaned radiometer, also known as the light-mill, in 1873, it was believed that this device confirmed the existence of linear momentum carried by photons[1], as predicted by Maxwell's equations. Although Reynolds later proved that the torque on the radiometer was caused by thermal transpiration[2], researchers continued to search for ways to take advantage of the momentum of photons and to use it for generating rotational forces. The ability to provide rotational force at the nanoscale could open up a range of applications in physics, biology and chemistry, including DNA unfolding and sequencing[3–6] and nanoelectromechanical systems[7–10]. Here, we demonstrate a nanoscale plasmonic structure that can, when illuminated with linearly polarized light, generate a rotational force that is capable of rotating a silica microdisk that is 4,000 times larger in volume. Furthermore, we can control the rotation velocity and direction by varying the wavelength of the incident light to excite different plasmonic modes.

Photons have both linear and angular momentum, and the influence of one or both becomes evident during scattering or absorbing processes. For example, the transfer of linear momentum from photons to an object results in an optical force that can be used for optical trapping[11] and cooling[12]. Also, the angular momentum carried by photons can induce a mechanical torque via scattering or absorbance, as first demonstrated by Beth more than 70 years ago[13].

The ability to generate significant optical torques at the nanoscale will benefit applications such as mechanical transducers and actuators, energy conversion and *in vivo* biological manipulation and detection. So far, however, the weakness of light–matter interactions (caused by the small optical constants of dielectric materials) means that micrometre- or even millimetre-sized motors are needed to generate a useful amount of torque. Moreover, most of these dielectric systems require manipulation of either the polarization state or the phase front of the illuminating beam to generate optical angular momentum. This limits both the torque switching time and the type of light sources and materials that can be used[11]. The interactions between light and matter can be made stronger by taking advantage of the enhancement of the electromagnetic field that occurs when it is resonant with the plasmons in a metallic nanostructure. Enhancement is therefore widely used in single-molecule detection and surface-plasmon enhanced Raman spectroscopy (SERS)[14–16].

Here, we propose and experimentally demonstrate a nanoscale plasmonic motor directly driven by light, in which its rotation speed and direction are controlled by tuning the frequency of the incident wave. We show that a single plasmonic motor, only 100 nm in size, can generate a torque that is sufficient to drive a micrometre-sized silica disk (4,000 times larger in volume) in water, owing to its strong interaction with light. Furthermore, such plasmonic motors can be coherently summed up in motor arrays, resulting in an increased induced torque and faster rotation of the microdisk[17]. This torque results solely from the symmetry of the designed plasmonic structure and its interaction with the light. It does not require any predetermined angular momentum of the light, so the illuminating source can be a simple linearly polarized plane-wave or Gaussian beam.

Light-induced rotation is obtained by careful design of the phase retardation induced by the electron inertia[18,19] and experienced by the light incident on a metallic structure (see Supplementary Information). The phase retardation can be engineered to vary within the structure, inducing orbital angular momentum on the scattered light that, in turn, results in a torque imposed on the sample. In other words, as a result of the conservation of angular momentum, an impetus with the opposite sign is applied to the plasmonic structure and provides the driving torque.

To take advantage of the light-induced torque, we shaped the plasmonic motors as planar gammadion gold structures that can be viewed as a combination of four small LC-circuits for which the resonant frequencies are determined by the geometry and dielectric properties of the metal[18,20–22]. Figure 1 presents a schematic of a single nanosized motor embedded in a squared silica microdisk and the corresponding scanning electron microscopy (SEM) image of the fabricated structure. This motor can strongly interact with light, giving rise to strong photon scattering and absorption[23]. In particular, at frequencies close to the plasmonic resonance, the light forms a unique plasmonic mode with distinct phase retardations between the currents at the different parts of the gammadion. This induces a similar phase pattern in the re-emitted light, which produces the opposite orbital angular momentum at the motor. Hence, the strongest optically induced torque is expected at these plasmon resonance frequencies.

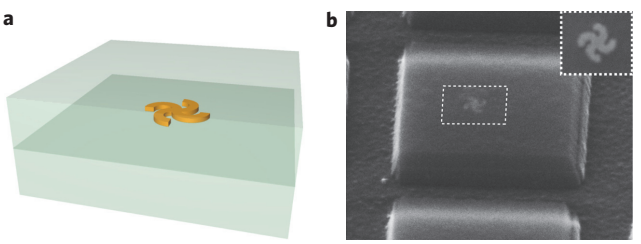

Figure 1 | Nanometre-scale plasmonic motor. a, Illustration of the nanosized gold motor, sandwiched between two identical 300-nm-thick square-shaped silica microdisks with an area of 2.2 × 2.2 μm^2. The large silica disk significantly reduces the Brownian motion of the particles (see Supplementary Information), so the rotation of the disk, induced solely by the subwavelength-sized motor, can be detected by optical far-field measurements. Furthermore, the two silica disks, in the centres of which are embedded the motors, ensure a mirror symmetric environment. **b**, SEM image of a silica disk including the plasmonic motor. The inset shows a magnified top view of the plasmonic motor (marked by dashed lines). The motor (radius, 100 nm; line width, 38 nm; thickness, 30 nm), is embedded in the centre of the silica disk.

[1]NSF Nano-scale Science and Engineering Center (NSEC), 3112 Etcheverry Hall, University of California, Berkeley, California 94720, USA, [2]Material Sciences Division, Lawrence Berkeley National Laboratory, Berkeley, California 94720, USA. *e-mail: xiang@berkeley.edu

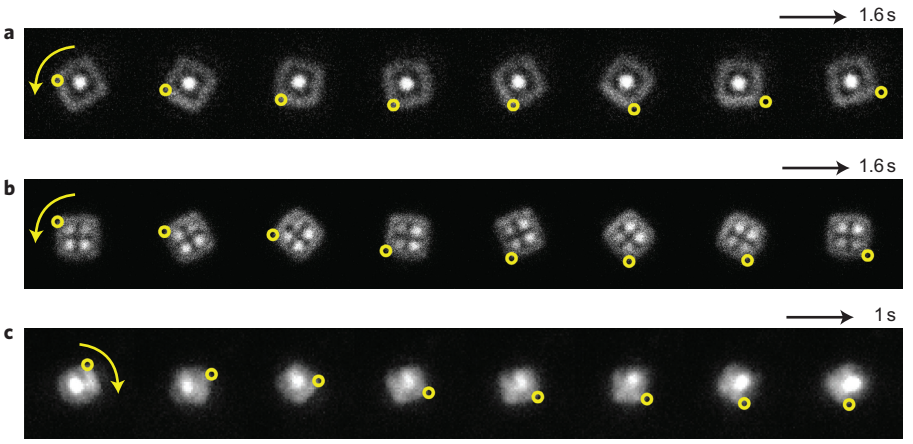

Figure 2 | Sequencing dark-field microscopy images of a rotating silica microdisk, driven by plasmonic motors. a, A single motor illuminated by a $\lambda_1 = 810$ nm laser beam causes the larger silica microdisk to rotate in an anticlockwise direction. **b**, A 4-in-1 motor sample rotates anticlockwise under excitation at a wavelength of 810 nm. Although they rotate at similar speeds, the 4-in-1 sample needs only half the light power required by the single-motor sample, which indicates that a stronger torque can be achieved by integrating more motor structures into one device. **c**, A laser beam with a wavelength of $\lambda_2 = 1{,}700$ nm induces a clockwise rotation for the same disk as in **a**. The total times for the three series are 1.6 s, 1.6 s and 1 s in sequence, with laser powers 1 mW, 0.5 mW and 3 mW, respectively. The beams were generated by a femtosecond Ti:sapphire oscillator and a synchronously pumped optical parametric oscillator, respectively. The bright spot in the centre of the silica disk results from strong scattering from the plasmonic motor, although the fine details of the structure cannot be observed by optical microscopy due to the diffraction-limited resolution. The silica disks are trapped by the same light beam.

Figure 2 presents sequencing images of the microdisk (in deionized water) rotated by a linearly polarized Gaussian beam. Figure 2a shows a single plasmonic motor (radius, 100 nm) rotating a 2.2×2.2-μm^2 disk when illuminated by a beam with a power of 1 mW at a wavelength of 810 nm, focused by an objective lens with a numerical aperture (NA) of 0.5. The disk rotates at 0.3 Hz anticlockwise (see real-time movie in the Supplementary Information). When multiple motors are integrated into one silica microdisk, the torques applied on the disk from the individual motors accumulate and the overall torque is increased[17] (see Supplementary Information). This is demonstrated in Fig. 2b, in which a silica disk with four motors attains the same rotation speed with only half of the laser power applied.

Interestingly, the rotation direction of the motor can be controlled merely by changing the wavelength of the light. When illuminated with a similar linearly polarized Gaussian beam but at a wavelength of 1,700 nm, the same single motor rotates clockwise (Fig. 2c; see also movie in the Supplementary Information). In other words, the rotation is a direct result of torque generated by different plasmonic modes arising from the interaction between the light and the motor, and does not stem from a predetermined angular momentum of the light, nor from a plasmonic heat effect inducing water flow (see Supplementary Information).

The dependence of the direction of rotation on the illumination wavelength can be understood by calculating the local electric field and the time-averaged Poynting vector generated on the motor when illuminated at different wavelengths (Fig. 3a,b). Different plasmonic modes can be excited at the motor by illumination at different wavelengths, which, in turn, drive different types of light–matter interactions. The inertia of the conduction electrons in the metal causes phase retardation between the currents at different parts of the gammadion (see Supplementary Information). Consequently, the amplitude and orientation of the Poynting vector induced in the motor depend on the illumination wavelength, and the generated optical torque is maximized at the resonance frequencies where the phase shift between the specific 'arms' of the gammadion is equal to $\pm\pi/2$. At an illumination wavelength of 810 nm (Fig. 3a), the Poynting vector is found to have two components: centripetal forces at the centre of the gammadion and tangential forces at the outer parts of the gammadion arms. Although the centripetal forces do not contribute to the torque, the tangential forces exerted on the arms provide a torque that drives the motor anticlockwise. At a wavelength of 1,700 nm (Fig. 3b), the second plasmonic mode is excited, and the Poynting vector is mostly concentrated in the gap between the metallic arms. The non-centripetal orientation of the forces provides a torque that rotates the motor clockwise. Figure 3c shows the torque calculated over the entire 600–2,400 nm wavelength range. The peak at the visible range and the dip at the near-infrared correspond to the positive (anticlockwise) and negative (clockwise) torques, respectively, resulting from the enhanced scattering near the two plasmonic resonances of the metallic nanostructure. The strong electric field enhancement at the IR resonance (blue curve) drives the large negative torque (black curve), which is clearly stronger than the positive torque at 810 nm. This explains the difference in observed rotation velocities in the single-motor experiment shown in Fig. 2a,c, which is further confirmed by measurements of the disk rotation at different frequencies around the resonances with 25 motors integrated into a silica disk (Fig. 3d). The large number of motors enhances the rotation speed to enable torque measurements even at off-resonance frequencies where the plasmonic response is weak (see Supplementary Information).

The correlation between the plasmon resonances and the light-induced torque is clearly observed in the relation between the measured transmission spectrum (Fig. 3e) and the frequency-dependent angular velocity of the rotated sample (Fig. 3d), where the resonance frequencies for which the absorption is strongest are found to be the same as those exhibiting the maximum rotation speed. Note that such a closely packed array of plasmonic elements exhibits strong coupling between the modes of the individual motors when the spacing between the motors (100 nm) is much smaller than the light–motor interaction cross-section (~600 nm; ref. 23). This results in a transition from a single resonance to an absorption 'band', most pronounced for the fundamental resonance around 1,500 nm, where the strong coupling results in additional higher-energy modes (see Supplementary Information). This additional evidence shows that the torque indeed originates from the plasmonic resonance.

The optical torque exerted on the silica disk can be found from the measured angular velocity using the classical equation of motion

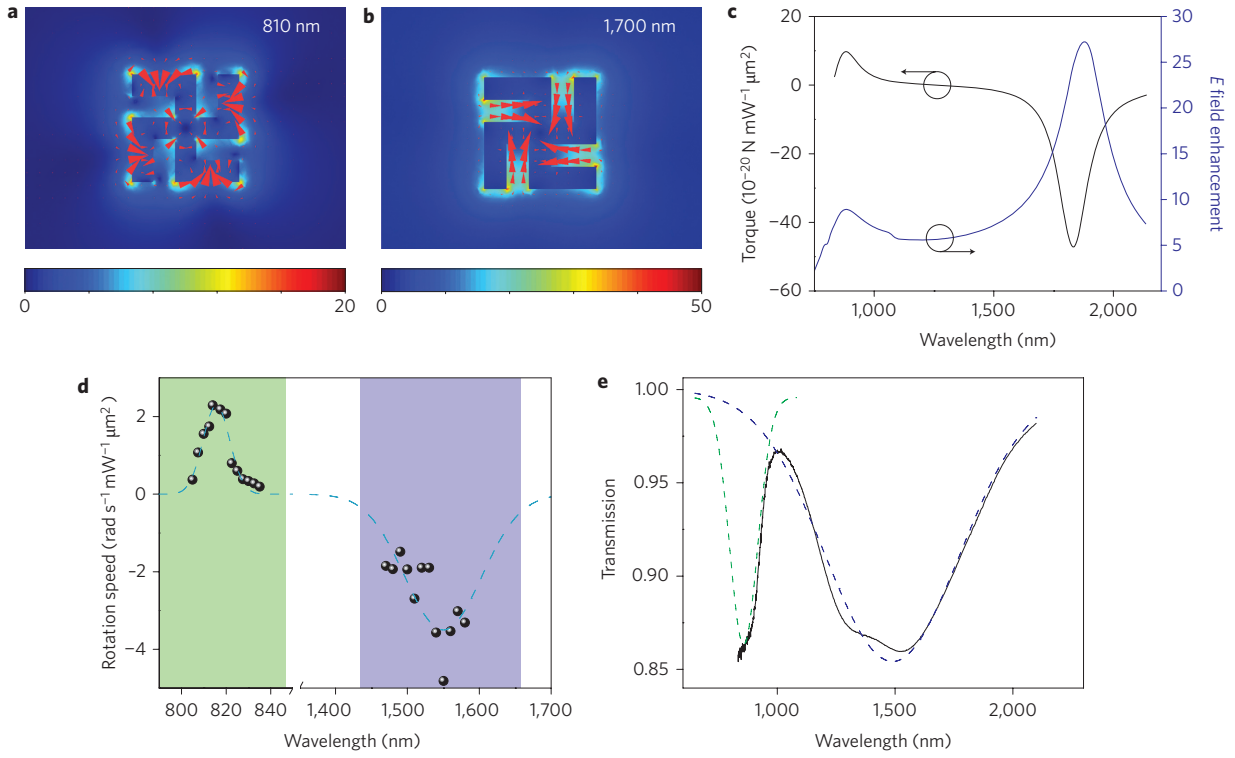

Figure 3 | Rotation characteristic and optical properties of the motors. a, Electric field and Poynting vector induced on the motor at an illumination wavelength of $\lambda = 810$ nm. The colour map shows the normalized electric field distribution, and the red arrows indicate the Poynting flux, which is proportional to the linear momentum of light in the vicinity of the motor. The Poynting flux is scattered/absorbed at the outer side of the arms, inducing a torque on the motor to drive it anticlockwise. **b**, The same as in **a** but for illumination at $\lambda = 1{,}700$ nm. The Poynting flux passes through the gaps and is scattered/absorbed by the elbow of the motor, providing a clockwise torque on the latter. **c**, Torque calculations on a single motor show positive and negative torques at the plasmonic resonance peak frequencies, which are indicated by the calculated electric-field enhancement at the gap. **d**, Measured variation of the rotation speed with wavelength of the excitation beam for a 25-in-1 motor sample. Positive rotation in the green area corresponds to anticlockwise rotation, and vice versa in the purple area. Dashed line is the fitting of the experiment data. **e**, Transmission spectrum of a 25-in-1 motor sample, measured by Fourier transform infrared spectroscopy (FTIR). The solid line corresponds to the measured spectrum and the dashed lines have been added to fit the spectrum, with the two resonant dips corresponding to the two plasmonic modes, one in the visible range (green) and the other in the near-IR (purple).

$I(\mathrm{d}\omega/\mathrm{d}t) + \gamma\omega = \tau_{\mathrm{motor}}$. Here, I is the momentum of inertia of the silica disk, ω is the rotation velocity, γ is a damping term originating from water viscosity, and τ_{motor} is the torque provide by the light–motor interaction. Because of the low Reynolds number in our system ($\sim 1 \times 10^{-5}$), the surface roughness and fine structures of the disk become insignificant, so it can be approximated as a cylindrical disk with radius a and a damping coefficient that becomes $\gamma = (32/3)\pi\mu a^3$, where μ is the water viscosity[24]. At steady state ($t \to \infty$), we obtain a single-motor torque of $\tau_{\mathrm{motor}} =$ 140 pN nm for 1 mW μm^{-2} incident intensity at the resonance wavelength, providing a driving power of 0.27 aW.

We have shown that a non-chiral nanoscale plasmonic element can provide an optical torque sufficient to rotate micrometre-sized dielectric samples when illuminated with a linearly polarized plane-wave or Gaussian beam. The unique plasmonic mechanism is manifested in an enhanced cross-section of the light–matter interaction and the ability to fully control the rotation speed and direction by merely tuning the illumination wavelength.

The demonstration of a mechanical torque driven by light opens exciting possibilities in nanoelectromechanical systems, energy conservation and biological applications, where the small motor size can make it useful for *in vivo* manipulation such as controlled winding and unwinding of DNA through illumination at different wavelengths. The range of applications for such motors can potentially be extended to solar light harvesting in nanoscopic systems by designing multiple motors to work at different resonance frequencies and single directions. Such multiple motor structures could be used to acquire torque from a broad wavelength range instead of a single frequency.

Received 13 April 2010; accepted 21 May 2010;
published online 4 July 2010

References

1. Crookes, W. Attraction and repulsion caused by radiation. *Nature* **12,** 125 (1875).
2. Reynolds, O. On certain dimensional properties of matter in the gaseous state. Part II. *Phil. Trans. R. Soc.* **170,** 727–845 (1879).
3. Allemand, J. F., Bensimon, D., Lavery, R. & Croquette, V. Stretched and overwound DNA forms a Pauling-like structure with exposed bases. *Proc. Natl Acad. Sci. USA* **95,** 14152–14157 (1998).
4. Bryant, Z. *et al.* Structural transitions and elasticity from torque measurements on DNA. *Nature* **424,** 338–341 (2003).
5. Abels, J. A., Moreno-Herrero, F., van der Heijden, T., Dekker, C. & Dekker, N. H. Single-molecule measurements of the persistence length of double-stranded RNA. *Biophys. J.* **88,** 2737–2744 (2005).
6. Gore, J. *et al.* DNA overwinds when stretched. *Nature* **442,** 836–839 (2006).
7. Fennimore, A. M. *et al.* Rotational actuators based on carbon nanotubes. *Nature* **424,** 408–410 (2003).
8. Judy, J. W. Microelectromechanical systems (MEMS): fabrication, design and applications. *Smart Mater. Struct.* **10,** 1115–1134 (2001).
9. Lehmann, O. & Stuke, M. Laser-driven movement of 3-dimensional microstructures generated by laser rapid prototyping. *Science* **270,** 1644–1646 (1995).
10. Eelkema, R. *et al.* Nanomotor rotates microscale objects. *Nature* **440,** 163 (2006).
11. Grier, D. G. A revolution in optical manipulation. *Nature* **424,** 810–816 (2003).

12. Kippenberg, T. J. & Vahala, K. J. Cavity optomechanics: back-action at the mesoscale. *Science* **321,** 1172–1176 (2008).
13. Beth, R. A. Mechanical detection and measurement of the angular momentum of light. *Phys. Rev.* **50,** 115–125 (1936).
14. Willets, K. A. & Van Duyne, R. P. Localized surface plasmon resonance spectroscopy and sensing. *Annu. Rev. Phys. Chem.* **58,** 267–297 (2007).
15. Kinkhabwala, A. *et al.* Large single-molecule fluorescence enhancements produced by a bowtie nanoantenna. *Nature Photon.* **3,** 654–657 (2009).
16. Maier, S. A. *et al.* Local detection of electromagnetic energy transport below the diffraction limit in metal nanoparticle plasmon waveguides. *Nature Mater.* **2,** 229–232 (2003).
17. Landau, L. D. & Lifshitz, E. M. in *Mechanics* Vol. 1 (Butterworth Heinemann, 1976).
18. Pendry, J. B., Holden, A. J., Robbins, D. J. & Stewart, W. J. Magnetism from conductors and enhanced nonlinear phenomena. *IEEE Trans. Microwave Theory Tech.* **47,** 2075–2084 (1999).
19. Gorodetski, Y., Niv, A., Kleiner, V. & Hasman, E. Observation of the spin-based plasmonic effect in nanoscale structures. *Phys. Rev. Lett.* **101,** 043903 (2008).
20. Rogacheva, A. V., Fedotov, V. A., Schwanecke, A. S. & Zheludev, N. I. Giant gyrotropy due to electromagnetic-field coupling in a bilayered chiral structure. *Phys. Rev. Lett.* **97,** 177401 (2006).
21. Shalaev, V. M. *et al.* Negative index of refraction in optical metamaterials. *Opt. Lett.* **30,** 3356–3358 (2005).
22. Linden, S. *et al.* Magnetic response of metamaterials at 100 terahertz. *Science* **306,** 1351–1353 (2004).
23. Husnik, M. *et al.* Absolute extinction cross-section of individual magnetic split-ring resonators. *Nature Photon.* **2,** 614–617 (2008).
24. Constantinescu, V. N. *Laminar Viscous Flow* (Springer, 1995).

Acknowledgements

This work was supported by the U.S. Department of Energy under contract no. DE-AC02-05CH11231 regarding simulations and fabrication, and by the NSF Nano-scale Science and Engineering Center (NSEC) under grant no. CMMI-0751621 for optical characterization.

Author contributions

M.L. and X.Z. developed the concept. M.L. designed and performed experiments and analysed the data. M.L. and Y.L. implemented the simulation. M.L., T.Z., G.B. and X.Z. discussed the results and wrote the manuscript.

Additional information

The authors declare no competing financial interests. Supplementary information accompanies this paper at www.nature.com/naturenanotechnology. Reprints and permission information is available online at http://npg.nature.com/reprintsandpermissions/. Correspondence and requests for materials should be addressed to X.Z.